

How common is the Milky Way - satellite system alignment?

Noam I Libeskind^{1,2}, Carlos S Frenk³, Shaun Cole³, Adrian Jenkins³ & John C Helly³.

¹*Racah Institute of Physics, Hebrew University of Jerusalem, Givat Ram, Jerusalem, Israel, 91904*

²*Astrophysikalisches Institut Potsdam, An der Sternwarte 16, Potsdam 14482, Germany*

³*Department of Physics, University of Durham, Science Laboratories, South Road, Durham, DH1 3LE, U.K.*

16 November 2018

ABSTRACT

The highly flattened distribution of satellite galaxies in the Milky Way presents a number of puzzles. Firstly, its polar alignment stands out from the planar alignments commonly found in other galaxies. Secondly, recent proper motion measurements reveal that the orbital angular momentum of at least 3, and possibly as many as 8, of the Milky Way’s satellites point (within 30 degrees) along the axis of their flattened configuration, suggesting some form of coherent motion. In this paper we use a high resolution cosmological simulation to investigate whether this pattern conflicts with the expectations of the cold dark matter model of structure formation. We find that this seemingly unlikely set up occurs often: approximately 35% of the time we find systems in which the angular momentum of 3 individual satellites point along, or close to, the short axis of the satellite distribution. In addition, in 30% of the systems we find that the net angular momentum of the 6 best aligned satellites lies within 35 degrees of the short axis of the satellite distribution, as observed for the Milky Way.

1 INTRODUCTION

The system of bright satellites orbiting in the halo of the Milky Way has a number of properties that seem unusual. Most of these satellites define a tight plane in the sky whose normal is roughly perpendicular to the Galaxy’s spin angular momentum vector (Lynden-Bell 1976; Kunkel & Demers 1976; Lynden-Bell 1982). In addition, this so-called *disc-of-satellites* (Kroupa, Thies & Boily 2005) appears to be well aligned with the orbital angular momentum of individual satellites, indicating some form of coherent motion (Metz, Kroupa, & Libeskind 2008).

The observed, highly anisotropic set-up is not an obvious outcome of the Λ CDM model in which the Universe is assumed to be composed primarily of cold dark matter (CDM) and vacuum energy associated with a cosmological constant (Λ). In this paradigm, structures form hierarchically via the merging of small subgalactic units formed out of the unstable overdense peaks of the initial matter density field. Satellite galaxies are identified with the substructures that survive the violent gravitational processes associated with

hierarchical growth. High resolution N-body simulations of galaxy formation have shown that small bound subhalos can survive these merging processes and that many remain as distinct substructures embedded in a present day galactic dark matter halo (e.g. Klypin et al. 1999; Moore et al. 1999; Diemand, Kuhlen & Madau 2007; Springel et al. 2008).

Before the flood of discoveries of new Milky Way satellites in the Sloan Digital Sky Survey (SDSS) (Willman et al. 2005; Belokurov 2006a,b; Zucker 2006a,b), it had been known for at least 3 decades that rather than being isotropically distributed in space, the 11 most luminous ‘classical’ satellite galaxies of the Milky Way are all aligned along a great circle on the sky (Lynden-Bell 1976; Kunkel & Demers 1976). Metz, Kroupa, & Jerjen (2009) have argued that the newly discovered SDSS satellites also lie on or close to this great circle. This ‘galactic pancake’ (Libeskind et al. 2005) of satellites was found to be aligned roughly perpendicular to the plane of the disc of the Milky Way (Lynden-Bell 1982). This particular set-up may be related to the “Holmberg effect,” the tendency for satellites of extragalactic systems

to be preferentially distributed along a specific direction. A number of studies (Holmberg 1969; Zaritsky et al 1997; Sales & Lambas 2004; Brainerd 2005; Yang et al 2005) have detected some alignment of satellite galaxy systems relative to their hosts, but disagree on the nature of its orientation. Holmberg (1969) and Zaritsky et al (1997) found “Milky Way” type alignments (i.e. polar, with satellites avoiding the equatorial regions), while planar alignments (i.e. with satellites avoiding the polar regions) have been observed in the 2-degree-field Galaxy Redshift Survey (2dFGRS, Colless et al. 2001) by Sales & Lambas (2004) and, in the SDSS, by Brainerd (2005) and Yang et al (2005).

Kroupa, Thies & Boily (2005) argued that the anisotropic nature of the distribution of the Milky Way’s satellite population contradicts the expectations of the Λ CDM model since the simple hypothesis that satellite galaxies are a random subsample of the entire subhalo population would imply near isotropy. However, recent numerical studies of the formation of satellites in the Λ CDM cosmology (Libeskind et al. 2005, 2007; Kang et al. 2005; Zentner et al. 2005) have found that there is not a one-to-one match between the brightest satellites and the most massive subhalos and indeed that the satellite galaxies are not a random subsample of the background subhalo population. Instead, the most luminous satellites populate the subset of subhalos which were the most massive before they were accreted. These studies also suggested that the tendency for satellites to align themselves in a great pancake may be a generic result of infall along filaments that form in the hierarchical buildup of a galactic halo or of accretion in groups (Li & Helmi 2008). This kind of coherent motion should perhaps also be reflected in the kinematics of the satellite galaxies.

Proper motions for some of the Milky Way’s satellite galaxies (at the level of milliarcsec/yr) have now been measured using both ground- (Scholz & Irwin 1994; Ibata et al. 1997; Dinescu et al. 2004, 2005; Schweitzer et al. 1995, 1997) and space-based telescopes (i.e. HST Kallivayalil, van der Marel & Alcock 2006; Kallivayalil et al. 2006; Piatek et al. 2003, 2005, 2006, 2007). Using these data, Metz, Kroupa, & Libeskind (2008) calculated the orbital angular momentum of 6 satellites. Remarkably, they found the angular momentum vectors of the satellites to be well aligned, generally pointing in the same direction, within 30 degrees, on the sky. This effect was not seen in the simulations of (Libeskind et al. 2005, 2007) which were shown to be consistent with a random orientation for the satellites’ angular momenta. This conclusion, however, was based on a very small sample of simulations of Milky-Way systems.

In this study we use a high resolution simulation of a large cosmological volume to explore the alignment of the positions and angular momenta of satellites in dark matter halos. With a much large sample than those previously con-

Table 1. Parameters of the hMS N-body simulation. (1) Box size (in h^{-1} Mpc); (2) number of particles; (3) dark matter particle mass (in M_{\odot}); (4) mean matter density; (5) vacuum energy density; (6) Hubble constant (in units of $100 \text{ km s}^{-1} \text{ Mpc}^{-1}$); and (7) normalization of the matter power spectrum.

l_{box}	N	m_{dm}	Ω_{m}	Ω_{Λ}	h	σ_8
100	7.29×10^8	1.3×10^8	0.25	0.75	0.73	0.9

sidered, we are able to investigate these properties with a high degree of statistical significance.

2 METHODS

2.1 N-body simulation and semi-analytic model

The parameters of the hMS Λ CDM N-body simulation that we analyze (listed in Table 1) are the same as the *Millennium Simulation* (Springel et al 2005) except that the box size is smaller and the mass resolution approximately ten times better (see Gao et al. 2008, for details). The simulation was performed using the L-GADGET2 code (Springel 2005) on 128 processors at the Cosmology Machine of Durham University’s Institute for Computational Cosmology. The simulation was populated with ‘galaxies’ using the semi-analytical model of Bower et al. (2006) applied to halo merger trees extracted from the simulation.

Large high-resolution simulations such as ours resolve a wealth of gravitationally bound substructures inside larger objects. When a small halo is accreted by a larger one, tidal stripping causes the substructure to lose mass, while dynamical friction against the parent halo’s background material causes its orbit to spiral in towards the centre. In order to identify and follow these accreted substructures we use the algorithm SUBFIND (Springel et al. 2001), which uses an excursion set approach recursively to identify local maxima in the dark matter density field. The extent of a substructure is then determined by locating saddle points in the dark matter density field. The gravitational binding energy is calculated and unbound particles are rejected. Finally a 20 particle lower limit is imposed on the substructures.

We identify subhalos at all redshifts in the simulation and use them to build halo merger trees which describe the hierarchical build up of structures (see Harker et al. 2006, for a full description). The trees provide the backbone for modelling the evolution of the baryons. We use the Durham semi-analytic galaxy formation model, GALFORM (Cole et al. 2000; Benson et al. 2002; Baugh et al. 2005), as extended by Bower et al. (2006) which, in brief, includes the following physical processes: (i) shock-heating and virialization of halo gas; (ii) radiative cooling of hot halo gas onto a galactic disc; (iii) star formation from cool gas in the disc

and during starbursts in the bulge; (iv) the evolution of stellar populations; (v) photoionization and its effect on the thermal properties of the intergalactic medium; (vi) reheating and expulsion of cooled gas due to feedback processes associated with supernovae, stellar winds and AGN; (vii) chemical evolution of gas and stars; (viii) reddening due to dust absorption; (ix) galaxy mergers; (x) formation of black holes in the bulges of galaxies via the accretion of gas during mergers and disc instabilities; (xi) the evolution of the size of bulges and discs;

2.2 The satellite sample

The semi-analytic model produces a galaxy catalogue at each simulation output. Resolution tests, in which we increased the minimum halo mass used in the merger trees, indicate that our catalogues are complete for satellite galaxies with V -band magnitude brighter than -8 . In the Milky Way, this magnitude limit corresponds to the 11th brightest satellite, (Draco, which has $M_V = -8.8$; see Mateo 1998). Although the number of known dwarf galaxies orbiting in the Milky way halo has increased by at least 15 in the past 3 years, as new local group dwarf satellites have been discovered in the SDSS, all of the newly discovered galaxies are faint and fall below our magnitude limit. For this reason, we do not consider them in this paper. (Note that the newly discovered SDSS satellites are spatially biased because of the limited sky coverage of the SDSS so it is unclear how their properties compare with those of the classical satellites.) Thus, when comparing with observations of the Milky Way satellite system we only consider the 11 classical satellite galaxies whose luminosity is greater than our magnitude limit.

In order to identify central galaxies that resemble the Milky Way, we apply a halo mass cut which excludes galaxies residing in haloes of mass $\leq 2 \times 10^{11} M_\odot$ and $\geq 2 \times 10^{12} M_\odot$. To refine further the search for Milky Way-type galaxies, we also apply a luminosity cut to eliminate central galaxies fainter than -20 in the V band. We consider only systems that contain 11 or more satellites within the halo virial radius, r_{vir} , defined as the distance from halo centre within which the mean interior density is 200 times the critical density.

In order to prevent contamination of an alignment signal by nearby central galaxies, we impose the isolation criteria shown schematically in Fig. 1. We eliminate for the galaxy catalogue any two central galaxies A and B that lie within each other's virial radius (Case I). If galaxy B lies within the virial radius of another galaxy A, we eliminate both from our sample if B has a stellar mass greater than that of A (Case II), and turn B into a satellite of A if it is less massive than A (Case III). In practice, cases I, II and III are rare with only 29, 63 and 102 galaxies falling into these categories respectively.

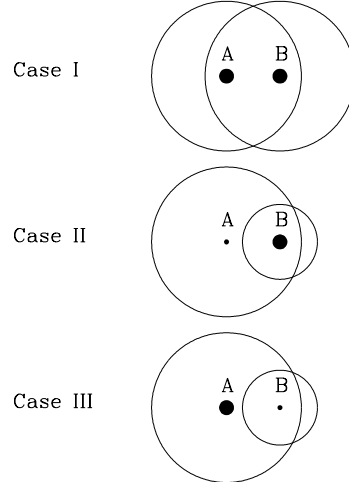


Figure 1. Isolation criteria. In case I (*top*), galaxy A is within galaxy B's virial radius and galaxy B is within galaxy A's virial radius; in this case both galaxies are eliminated from the sample. In case II (*middle*), galaxy B lies within galaxy A's virial radius (but not vice-versa) and galaxy B is more massive than galaxy A; in this case both galaxies are eliminated from the catalogue. In case III (*bottom*), galaxy B is within galaxy A's virial radius and is less massive than galaxy A; in this case galaxy B is regarded as a satellite of galaxy A.

When applied to the galaxy list produced by the semi-analytic model, the halo mass cut leaves us with 30 946 systems. The central galaxy magnitude cut reduces our sample to 3 230 halos, while the isolation criteria leaves us 3 201 systems. This sample is further reduced to 436 galaxies which possess at least 11 satellites. The median halo masses of each sample after these 4 cuts are $10^{11.32}$, $10^{11.82}$, $10^{11.82}$ and $10^{11.96} M_\odot$ respectively. Thus the median halo mass is only increased by 38% by the requirement that each system host at least 11 satellites.

3 SATELLITE GALAXY ALIGNMENTS

We first consider the alignment between satellite galaxy systems and the shape of the parent halo and then investigate the alignment of the satellites' orbital angular momentum vectors.

3.1 Orientation of the halo and satellite positions

Once the isolation criteria, and mass and luminosity cuts have been applied we obtain a list of central galaxies. We wish to examine the flattening of both their haloes and satellite systems. To do so, we first define the inertia, or second moments tensor,

$$I_{j,k} = \sum_i x_{j,i} x_{k,i}, \quad (1)$$

where we sum either over all the particles or all the satellites in the halo. We diagonalize this tensor and obtain the principal axes of the system, defined conventionally such that $a > b > c$. Previous studies (e.g. Bullock, Kravtsov & Weinberg 2000; Libeskind et al. 2005, 2007) have shown that although haloes tend to be mildly aspherical, their satellite populations exhibit a much more pronounced flattening. In order to verify this with our sample, we calculate the eigenvalues of the inertia tensor for the dark matter particles in each halo and for the systems of 11 brightest galaxies within r_{vir} .

The flattening of the haloes in our sample is evident in Fig. 2 where we plot c/a versus b/a . From the definition of a , b and c , no points may lie in the triangular upper half of this plot. The mild asphericity of our sample is reflected in the tendency for haloes to occupy the upper right area of Fig. 2. The median values of these halo axial ratios are $\langle b/a \rangle = 0.87$ and $\langle c/a \rangle = 0.77$.

The mild asphericity of dark matter haloes may be contrasted with the much more flattened configurations defined by their satellite systems, as shown in Fig. 3. This sample shows a much broader distribution of axial ratios, and contains many more examples of very triaxial systems than the halo population. The median values of the axial ratios are significantly smaller than for the halo sample, with $\langle b/a \rangle = 0.69$ and $\langle c/a \rangle = 0.43$.

The nature of the satellite’s aspherical distribution is related to the fact that satellites do not simply trace the background dark matter, but occupy biased positions in the halo closer to the principal axes. We assess the significance of this effect by conducting a “randomization” test of the null hypothesis that satellites are randomly drawn from the dark matter distribution. For each satellite in a halo, we randomly select a dark matter particle at the same radius. We then proceed to calculate the principal axes for both the satellite systems and those consisting of the random particles replacing each of the 11 brightest satellites.

We use these two sets of principal axes to project the location of each satellite and its random counterpart onto a Hammer-Aitoff projection of the whole sky, shown in Fig. 4. The upper panels show the location on the sky of the model satellites. For each central galaxy, we plot the positions of its satellites rotated onto the reference frame defined by the *disc-of-satellites* of the 11 brightest satellites. By definition, the satellites will concentrate along the long axis, a feature readily visible in the upper panels of Fig. 4. However, the

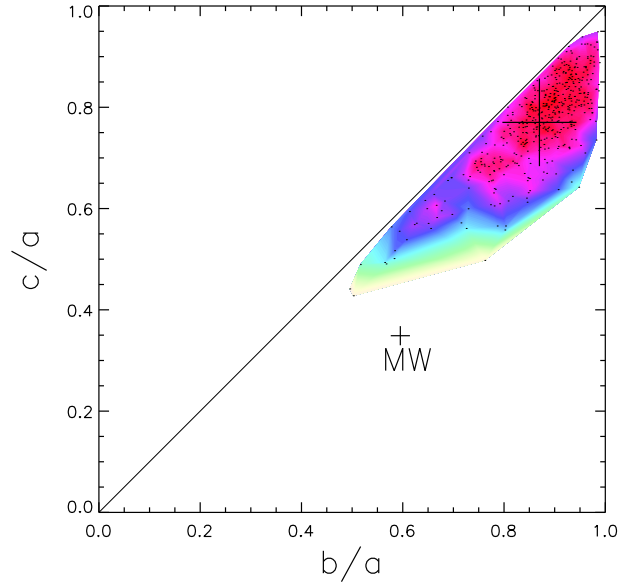


Figure 2. The ratio of short-to-long axis *versus* the ratio of intermediate-to-long axis for our halo sample. Each halo is shown as a black point while contours represent the density of points on an arbitrary scale, with red being the highest density and white the lowest. The large plus sign marks the median value of $(b/a, c/a)$ and its arms represent the 1σ extent of haloes in either direction. The point marked “MW” indicates the location on such a plot of the Milky Way’s *disc-of-satellites*

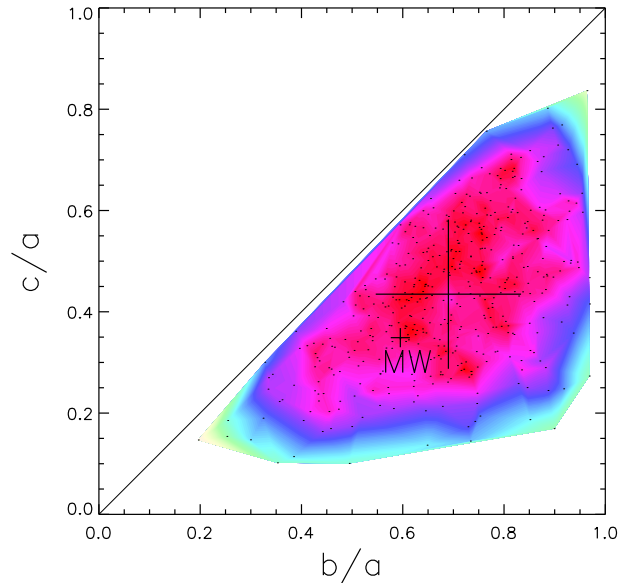


Figure 3. Same as Fig. 2, but for our sample of halo satellites.

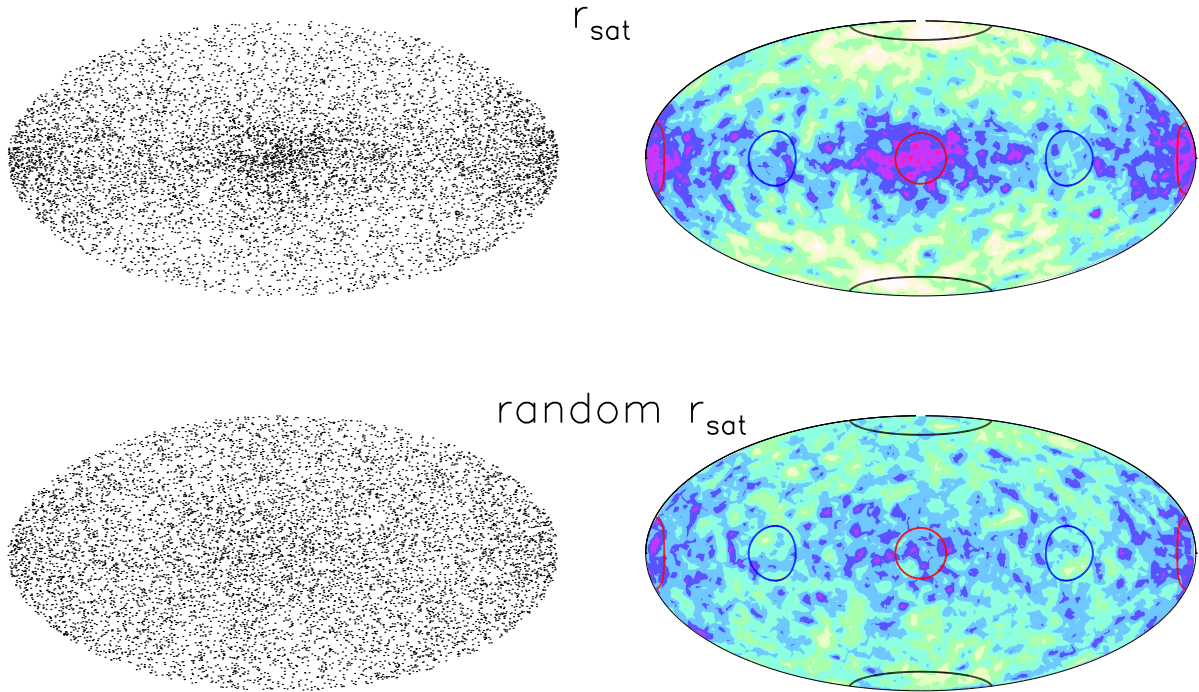


Figure 4. *Upper panel:* the location on the sky of all satellites in our halo sample, rotated into the frame defined by the satellite system’s principal axes. On the left we plot the position of each satellite, while on the right we show a false-colour map of satellite galaxy “density” (defined using the angular distance to the 10th nearest neighbor). High density regions are indicated by the purple/red shading, while less dense regions are indicated by the white shading. The red, blue, and black circles define areas within 15 degrees of the a , b and, c axes. *Bottom panel:* as above but for “randomized” satellites.

total fraction of satellites that lie close to the long axis is determined by the strength of the intrinsic flattening.

We can compare the upper panels of Fig. 4 to the lower panels which show the location on the sky of the random particles that replaced the brightest satellites projected onto the reference frame defined by those replacing the 11 brightest in each halo. These particles also tend to be aligned with the long axis of their distribution (by construction), but to a lesser extent than the model satellites. The pseudo-*disc-of-satellites* defined by the randomly selected dark matter particles is visibly less aspherical than the true *disc-of-satellites* defined by the 11 brightest satellites in each halo.

We can quantify this behavior by plotting a histogram of the angle between the position vector of each satellite (\hat{r}_{sat}) and the short axis (for example) of the ellipsoid defined by the brightest 11 satellites (\hat{c}_{sat}). Fig. 5(a) shows that the model satellites (black lines) exhibit a much stronger perpendicular alignment with the short axis of their distribution than the corresponding set of random dark matter particles (red lines). A Kolmogorov-Smirnov test rejects the

hypothesis that these two distributions are drawn from the same parent distribution or from a uniform distribution at a very high confidence level (formal KS probabilities $\sim 10^{-37}$). Around 15% more model satellites lie further than 65 degrees from \hat{c}_{sat} than expected from the associated dark matter particles. We conclude that satellite positions are not a random sample of the halo and that satellite systems are significantly flatter than their parent halos.

It is straightforward to check the degree of alignment of the *disc-of-satellites* defined by the 11 brightest galaxies with their host halo. Fig. 5(b) shows the cosine of the angle between the short axis of the *disc-of-satellites* (\hat{c}_{DOS}) and the short axis of the host halo (\hat{c}_{halo}). The model discs-of-satellites (black line) show a clear tendency to be aligned with the main plane of the halo. Indeed, nearly 40% of all satellites systems fall in the last bin of the histogram. However, a non-negligible fraction of systems are not aligned, in the sense that their minor axes are nearly perpendicular to the halo’s minor axis. For example, approximately 10% of the model *discs-of-satellites* are mis-aligned by more

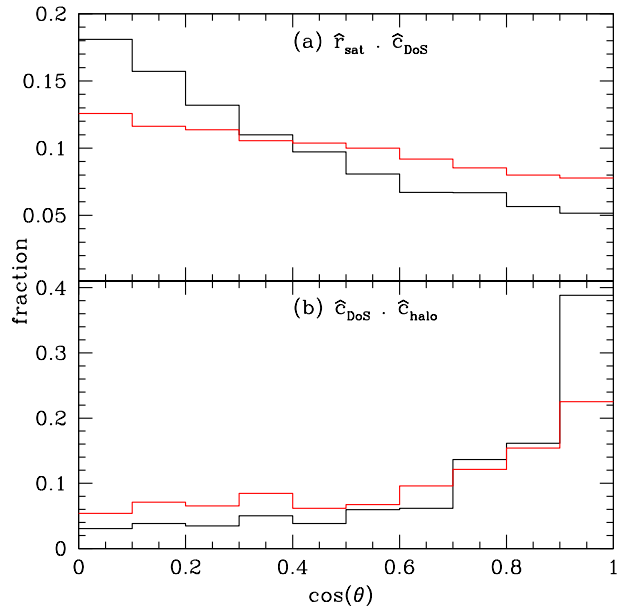


Figure 5. *Top panel:* (a) The distribution of the cosine of the angle between the short axis of the each halo’s satellite system ellipsoid and the position of each satellite galaxy (black curve). The red line shows the analogous distribution for the “randomized” sets of satellite galaxies. *Bottom panel:* (b) The distribution of the angle between the short axis of each halo’s dark matter distribution and the short axis of the *disc-of-satellites* composed of the brightest 11 satellite galaxies.

than 75° . To assess the significance of this trend, we define randomized *discs-of-satellites* using the set of dark matter particles replacing the brightest 11 model satellites. Again, a Kolmogorov-Smirnoff test rejects the hypothesis that the actual and randomized samples are drawn from the same parent distribution, or that either is drawn from a uniform distribution, at a very high confidence level.

3.2 Orbital angular momentum of satellites

A number of recent studies (e.g. Piatek et al. 2003, 2005, 2006, 2007, and other references in Metz, Kroupa, & Libeskind 2008) have obtained upper limits on the proper motion of eight of the Milky Way (MW) dwarfs. A detailed study of their angular momenta reveal two particularly interesting aspects of their orbital motion. The first is that the angular momentum vectors of at least 6 of these satellites point to within 30 degrees of the mean angular momentum vector of the set for which proper motions are available. The second is that the orbits of at least 5 satellites fall within 30 degrees of the normal of the *disc-of-satellites* defined by the 11 brightest dwarfs.

Metz, Kroupa, & Libeskind (2008) tested for these two properties in 6 simulations of MW-sized galaxy halos and found that in none of them did the satellites (identified in a similar manner as in this work) exhibit the same kind of coherent motion inferred for a subset of MW satellites. None of the 6 simulated haloes in that work had 5 satellites with with angular momentum vectors within 30 degrees of the normal to the fitted *disc-of-satellites*. Just 2 of the halos had 3 satellites whose angular momentum vectors fell within this region. In addition, the mean angular direction of the orbital poles of the simulated satellites did not lie close to the normal of the *disc-of-satellites*, in contrast to the MW.

Metz et al. concluded from this study that the dynamics of at least 5 “rotationally supported” MW satellites were (at least) hard to reproduce in CDM simulations. They suggested that the mismatch between the simulations and the observations could, in theory, be explained if the satellites of the MW had a different origin from those in the simulations, for example, if they were “tidal dwarfs”, formed in a tidal stream generated in a recent major merger (e.g. Metz & Kroupa 2007).

Our sample of MW type satellite systems is well suited to testing whether or not the orbital dynamics of satellites in Λ CDM simulations are consistent with the MW data. In Fig. 6 we show the location on the sky of the orbital angular momentum of each satellite (upper panels) and its randomized counterpart (lower panels) in our halo sample. We rotate each point on the sky into the frame defined by the principal axes of the “*disc-of-satellites*” defined either by the model satellites or by their randomized counterparts. There is an ambiguity in choosing which direction of the \hat{c}_{sat} axis to take to define the short axis. We choose the \hat{c}_{sat} axis to point in the direction which is closest to the mean angular momentum vector of each system. Therefore, the satellites that fall in the Southern hemispheres of Fig. 6 are counter-rotating with respect to the mean angular momentum of the *disc-of-satellites*.

Two features are readily visible in this figure. Firstly, the directions of the angular momentum of the randomized dark matter particles replacing the model satellites are much more uniform than those of the actual model satellites. Secondly (by construction), in both samples the distributions show an excess around the “North” pole, which is much more pronounced for the model satellites than for their randomized counterparts. On closer examination we note that, as well as the higher density around the North pole, there is a tendency for the angular momenta to point close to the $\hat{b}_{sat} - \hat{c}_{sat}$ plane. This effect may be produced by the radially biased orbits of the satellites in our sample. If a satellite lies along or near \hat{a}_{sat} , and if it is also moving close to this direction, its angular momentum vector will point somewhere on the $\hat{b}_{sat} - \hat{c}_{sat}$ plane.

Satellites have a much stronger tendency to display coherent orbital angular momenta than the background dark

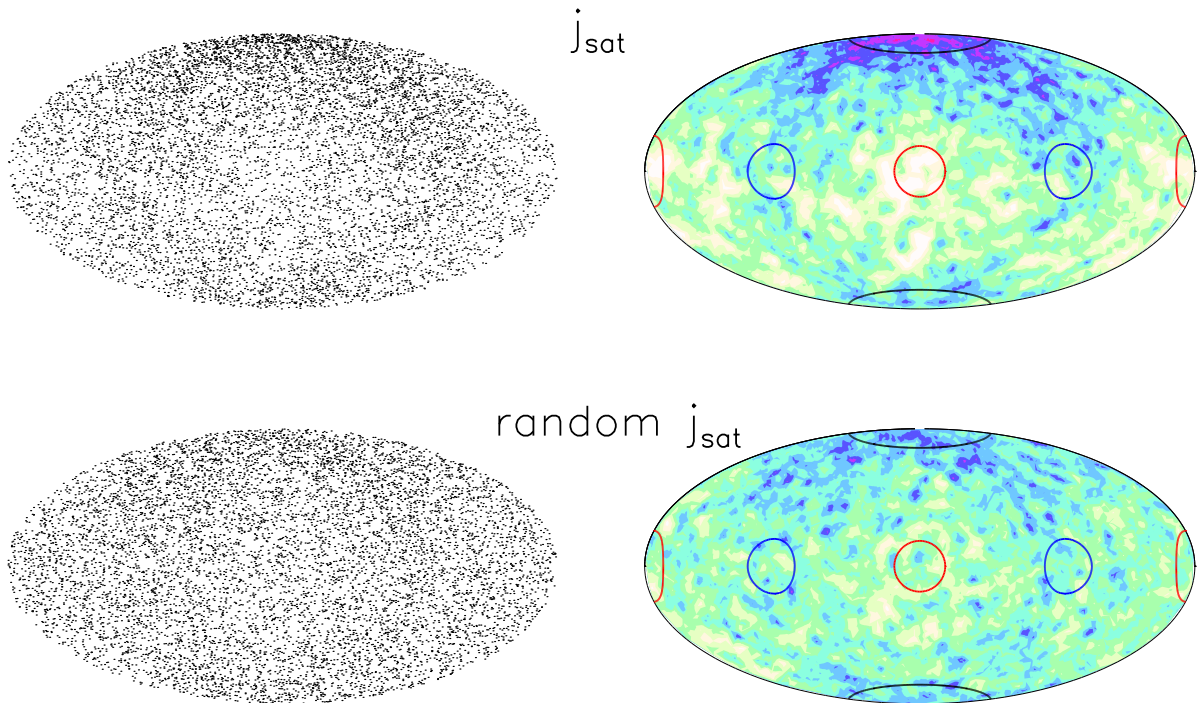


Figure 6. *Upper panel:* The location on the sky of the orbital angular momentum vector for all satellites in our halo sample, rotated into the principal axes of the disc-of-satellites. In these projections we choose from the two possible opposing directions for the c -axis the one which is closest to the mean angular momentum vector of the satellite sample. On the left we show the location of each satellite’s angular momentum vector, while on the right we show a contour map of satellite angular momentum “density” (defined by the angular distance to the 4th nearest neighbor). High density regions are indicated by the red/purple shading, while less dense regions are indicated by the white shading. The red, blue, and black circles define areas within 15 degrees of the a , b and c axis. *Bottom panel:* The same as above, but for randomized satellites.

matter. In Fig. 7 we show the distribution of the cosine of the angle between each satellite’s orbital angular momentum vector, j_{sat} , and \hat{c}_{sat} . This plot quantifies what is visually apparent in Fig. 6: an above random alignment between the orbital angular momentum of individual satellites and the short axis of the ellipsoid to which it belongs. The Kolmogorov-Smirnoff probability that the model satellites and the random particles are drawn from the same population is negligible.

Thus, our model satellites display the same kind of apparent coherent motion and spatial flattening as the real MW satellite system. Yet, the nature of this coherent motion is unclear. Metz et al. suggested that in the MW, the *disc-of-satellites* is supported purely by rotation. In this scenario, the majority of satellites move on circular orbits such that the *disc-of-satellites* itself is supported by the rotation of the galaxies orbiting in it. In order to test this hypothesis we carry out the following calculation. As in Fig. 6, we define

the z -axis to be parallel to the short (c) axis of the satellite distribution and of the two opposing directions this defines, we select the one closest to the direction of the mean angular momentum of the satellites. For each galaxy we calculate its angular momentum in this ‘ z ’-direction and call this quantity $J_z(E)$. We then estimate the angular momentum of a satellite with the same orbital energy, but on a purely circular orbit, $J_{zc}(E)$. If these two quantities are similar (i.e. $J_z(E)/J_{zc}(E) \approx 1$), then the satellite’s orbit must be approximately circular and rotationally supported. Note that since a circular orbit maximizes the angular momentum, the ratio $J_z(E)/J_{zc}(E)$ must always be ≤ 1 .

For each halo, we estimate its concentration assuming a Navarro, Frenk & White (1996; NFW) profile. Once we know the halo concentration, we use eqns (2.18) and (2.19) of Lacey & Cole (1996), together with the satellite’s radial position in the halo, to calculate its energy. We then search for the parameters (i.e. the distance and velocity) of a circu-

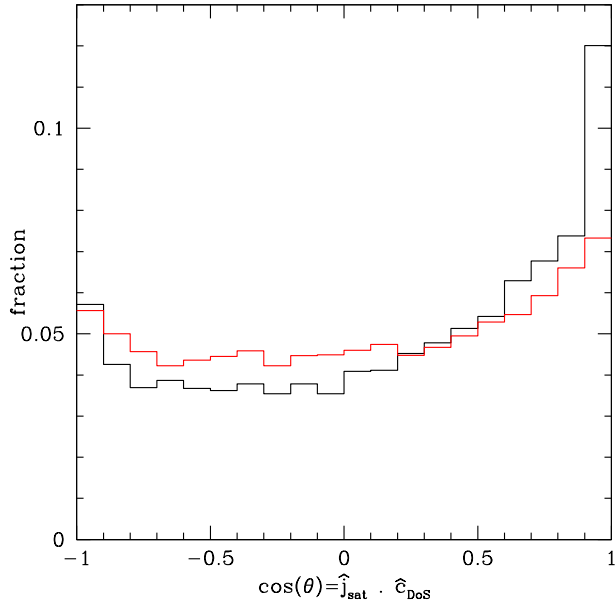


Figure 7. The distribution of the cosine of the angle between \hat{j}_{sat} , the satellite galaxy orbital angular momentum, and \hat{c}_{sat} (black lines). The red lines show results for the control sample of randomized dark matter particles.

lar orbit within an NFW potential with the same energy. In this way, we build the ratio $J_z(E)/J_{zc}(E)$ whose distribution we show in Fig. 8.

There are two salient points visible in Fig. 8. The first is that the distributions are not peaked at ≈ 1 , but rather at ≈ 0 , implying that $J_z(E) \ll J_{zc}(E)$. The majority of the satellites and their randomized counterparts are therefore *not* on circular orbits around the z -axis. It is interesting to note that the control sample exhibits a more pronounced symmetry about 0 than the satellite sample, implying similar numbers of counter- and co-rotating particles. The satellite sample, on the other hand, is somewhat skewed towards positive values of $J_z(E)/J_{zc}(E)$, implying that more satellites are co-rotating.

We now quantify how common the configuration of the satellite system of the MW is in our Λ CDM simulation. Of the 11 classical satellites in the MW, 8 (Sagittarius, Draco, Fornax, Ursa Minor, Carina, Sculptor the SMC and the LMC) have proper motion estimates which allow us to estimate the direction of their orbital angular momentum (e.g. see Table 2). Of these eight, the LMC, the SMC, and Fornax have angular momentum pointing well within 30 degrees of the direction to the normal of the plane fitted to the 11 classical satellites. The angular momentum vectors of an additional 2, Ursa Minor and Carina, have error bars large enough that they are compatible with a < 30 degrees mis-

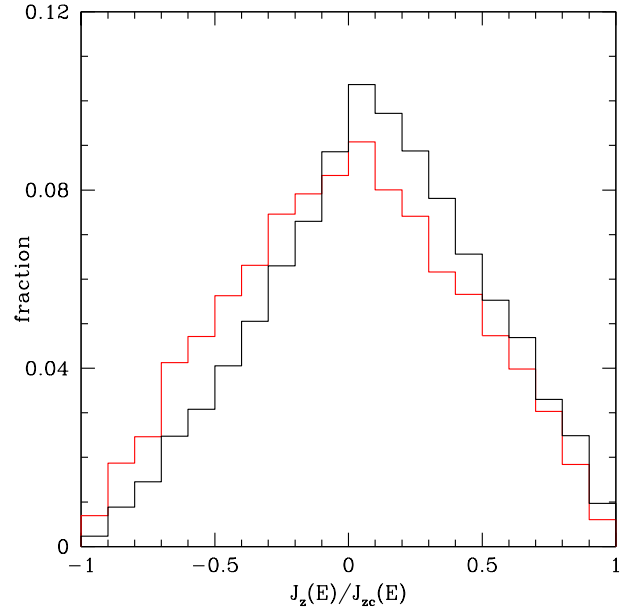


Figure 8. Histogram of the ratio of the z -component of the angular momentum of each model satellite, $J_z(E)$, to the angular momentum of a satellite on a circular orbit with the same energy, $J_{zc}(E)$ (black lines). If the *disc-of-satellites* were rotationally supported, all orbits would be circular and the distribution should be strongly peaked around ~ 1 . The red lines show the the histogram for the control sample of matched dark matter particles.

alignment with the pole. Additionally, there are 3 satellites without proper motion estimates, implying a minimum of 3 out of 11 ($\sim 27\%$) and a maximum of 8 out of 11 ($\sim 73\%$) satellites with angular momenta within 30 degrees of the perpendicular to the plane of the *disc-of-satellites*.

To assess how common this form of alignment is, we perform the following calculation: for each simulated halo with more than 11 satellites, we fit the standard plane to the 11 brightest, as described in Sec. 3.1. We then calculate how often the orbital angular momentum of N randomly selected satellites falls within 15, 30 or 45 degrees of \hat{c}_{sat} , where the direction of the \hat{c}_{sat} axis is chosen, as before, to be the one that is closest to the mean angular momentum vector. The results are shown in Fig. 9.

We find, for example, that the probability of finding at least 3 satellites within 30 degrees of \hat{c}_{sat} is around 35%, a similar number to that found in the simulations of Metz et al. If $n = 5$, this value drops to $\sim 5\%$. The probability varies rapidly with satellite number and the chance of finding 9 satellites within the specified angle (the total number of classical satellites - save Sagittarius and Sculptor - that could possibly be aligned) drops to 1%. The number of satellites with angular momentum aligned with the normal to the

Table 2. Census of the positions and angular momenta of the MW’s satellite population. Column 1 shows the satellite’s name. Column 2 gives the galacto-centric distance of each satellite. Column 3 gives the angular separation between the normal of the plane fitted to the Milky Way’s *disc-of-satellites* and the angular momentum vector of each satellite. Column 4 gives angular separation between the direction of the mean angular momentum of the 6 satellites moving in the most ordered fashion, J_{mean}^6 , to the angular momentum vector of each satellite. Columns 5 and 6 indicates whether the uncertainty in the measurements of the satellite galaxy’s angular momentum are consistent with placing the pole of the angular momentum vector within 30 degrees of the normal of the *disc-of-satellite*’s or within 35 degrees of J_{mean}^6 . For observational references see Metz, Kroupa, & Libeskind (2008) and references therein.

Name	d_{GC} (kpc)	$\Delta\phi_{\text{csat}}$ (deg)	$\Delta\phi_J$ (deg)	within \hat{n}_{DoS}	within J_{mean}^6
LMC	50	13	7	YES	YES
SMC	57	21	15	YES	YES
Fornax	140	23	25	YES	YES
Ursa Minor	68	38	18	YES	YES
Carina	103	49	61	YES	YES
Draco	82	69	55	NO	YES
Sagittarius	16	118	98	NO	NO
Sculptor	79	136	156	NO	NO
Sextans	86	–	–	unknown	unknown
Leo I	205	–	–	unknown	unknown
Leo II	250	–	–	unknown	unknown

disc-of-satellites also depends strongly upon cone angle. For example, we find 3 satellites within 45 degrees around 70% of the time but only 5% of the time within 15 degrees.

Metz, Kroupa, & Libeskind (2008) also remarked on the coherence of the angular momenta of the Milky Way’s satellites. They chose to omit 2 satellites (Sculptor and Sagittarius) as their angular momentum vectors point far from the mean and are clearly not members of a “common stream”. They then computed the mean angular momentum vector and its error for the remaining 6 satellites that have measured proper motions. Relative to this mean angular momentum direction, they found that a minimum of 4 (the LMC, SMC, Fornax and Ursa Minor) out of 11 ($\sim 36\%$), and a maximum of 9 out of 11 ($\sim 82\%$), satellites fall within the 35 degree error circle.

We perform a similar calculation to determine the probability of such an alignment. In order to mimic their procedure, for each halo we first calculate the net angular momentum of a randomly selected 8 satellites from the brightest 11. Then, after omitting the 2 satellites whose angular momenta are furthest from this mean, we compute the mean angular momentum vector of the remaining 6. We refer to this quantity as J_{mean}^6 . Although Metz, Kroupa, & Libeskind (2008) did not use this exact prescription, it is equivalent to theirs and it results in the same selection for the Milky Way. We

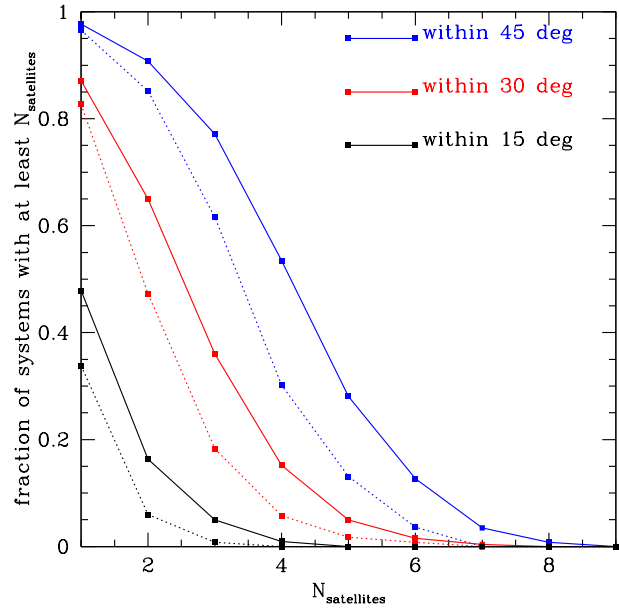


Figure 9. The fraction of systems in which the angular momentum of at least N satellites drawn from the brightest 11 lies within 15 (black), 30 (red), and 45 (blue) degrees of \hat{c}_{sat} (solid lines) and of J_{mean}^6 (dashed lines).

then calculate how often N randomly selected satellites fall within 15, 30 and 45 degrees of the direction of J_{mean}^6 . Our results are shown as the dotted lines in Fig. 9

We find that the arrangement in the Milky Way, where 4 satellites have angular momentum lying within 30 degrees of J_{mean}^6 , occurs reasonably frequently ($\sim 10\%$ of the time). However, we find that the probability of finding the maximum possible number of satellites (9) with angular momentum vectors pointing within the even larger angle of 45 degrees from J_{mean}^6 is negligible. If future proper motion measurements for the remaining 3 satellites (Sextans, Leo I and Leo II) reveal that they too are closely aligned with J_{mean}^6 , then our results suggest that such a setup would be extremely unlikely in our Λ CDM galaxy formation model.

Fig. 9 shows the probability that the orbital angular momentum of a random N out of 11 satellites falls close to the short axis of the *disc-of-satellites* or J_{mean}^6 . The mean orbital angular momentum of N satellites could still lie close to the axis (as in the MW), even if the angular momentum of the individual satellites are widely distributed. In Fig. 10a, we show the distribution of the angle between the mean orbital angular momentum of the 6 best aligned satellites, J_{mean}^6 , and the short axis of the *disc-of-satellites*, \hat{c}_{sat} .

Fig. 10a shows that there is an overabundance of systems that fall in the highest bin, corresponding to an angle of $\theta \lesssim 25$ degrees. The fraction of systems

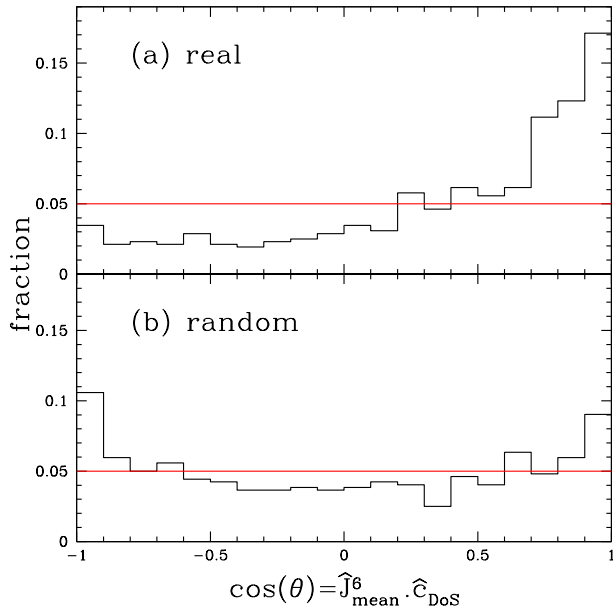


Figure 10. The distribution of the angle between the mean orbital angular momentum, J_{mean}^6 , of the 6 best aligned satellites and the short axis of the *disc-of-satellites*, \hat{c}_{sat} . We show the distribution for both the model satellites (a) in the upper panel, and for the associated randomized dark matter particles (b) in the lower panel. The dashed red line indicates a uniform distribution in $\cos(\theta)$.

whose J_{mean}^6 lies within 25 degrees of \hat{c}_{sat} is around 17%, well above the 5% expected for a uniform distribution. This is not an exceedingly large proportion, and although Metz, Kroupa, & Libeskind (2008) failed to find a single example in 6 simulations, our result - that such an alignment occurs roughly 17% of the time - is consistent with their findings. There is roughly a 50% chance of seeing such an alignment in just 1 out of 6 systems drawn at random from our sample. Yet, the non-uniformity of the distribution of the angle between J_{mean}^6 and \hat{c}_{sat} is statistically very significant: a Kolmogorov-Smirnoff test rules out the hypothesis that this sample is drawn from a random distribution at very high confidence.

We contrast these results with the histogram in the lower panel of Fig. 10b which shows the distribution of the same angle but now with J_{mean}^6 defined by the matched randomly selected control particles. In this case, the distribution is consistent with uniformity: the KS probability of drawing such a sample from a uniform distribution is roughly 20%. In other words, the orbital angular momentum of the control particles (which were chosen to be at the same radial distances as the model galaxies), exhibits

no preference for pointing near the normal of the plane they define.

4 CONCLUSION AND DISCUSSION

In this paper we have used a large cosmological N -body simulation of the Λ CDM cosmology, populated with galaxies using the GALFORM semi-analytic model of galaxy formation, to investigate the expected frequency of the peculiar alignments exhibited by the satellite galaxies of the Milky Way. We confirm previous work (e.g Kang et al. 2005; Libeskind et al. 2005; Zentner et al. 2005) which found highly flattened spatial distributions of satellites within the much more spherical dark matter distributions of simulated galactic halos. The satellite ellipsoid tends to be aligned with the shape of the dark matter halo, although in a small fraction of cases it is anti-aligned.

We have also used our simulation in an attempt to understand the dynamics of satellites within Milky Way type halos. We have found that systems that resemble the Milky Way - with at least 3 satellites orbiting within 30 degrees of the normal to the plane defined by the 11 brightest of them - occur roughly 35% of the time. This is consistent with the work of Metz, Kroupa, & Libeskind (2008) who found 2 out of 6 galaxies showing this behavior. However, the fraction of systems which have 8 satellites all orbiting with angular momentum aligned to within 30 degrees of the normal to their plane is less than 1.5% at the 95% confidence level. Thus, if reliable proper motion estimates for the remaining 5 ‘‘classical’’ Milky Way satellites reveal that they too orbit near this plane, this coincidence would be difficult to explain within our Λ CDM galaxy formation model. In roughly 17% of our simulated galactic halos we find systems in which the *mean* orbital angular momentum of the 6 best aligned satellites lies within 25 degrees of the short axis of the satellites’ plane (and, in 30% of cases within 35 degrees), as seen in the Milky Way.

The aligned satellites in the simulations do not make up a rotationally supported *disc-of-satellites*. Similarly, and contrary to the suggestion by Metz, Kroupa, & Libeskind (2008), the rough alignment of some of the MW’s satellites with the pole of their *disc-of-satellites* does not imply that the system is rotationally supported. This can only be ascertained by comparing the angular momenta of the satellites with the values for circular orbits of the same energy. Only this comparison (which requires various model assumptions) can expose how circular the orbits really are. If indeed the orbits of the Milky Way satellites turn out to be rotationally supported, this would be difficult to explain in the Λ CDM model.

The main result of this paper is the robust quantification of the fraction of Milky Way type galaxies in the Λ CDM cosmology that resemble our Galaxy as far as its anisotropic

satellite distribution and dynamics are concerned. While previous analysis of simulations (Libeskind et al. 2005, 2007; Zentner et al. 2005; Metz, Kroupa, & Libeskind 2008) have come to some of the same conclusions as we do here, their statistical significance was compromised by small sample sizes (6, 3, 3 and 6 haloes respectively). Our large sample of over 400 Milky Way sized haloes allows us robustly to quantify the expected frequency of both satellite flattening and coherent satellite motion.

Future surveys such as Pan-STARRS or SkyMapper (Kaiser et al. 2002; Keller et al. 2007) will obtain a more complete census of the Milky Way’s satellite population, including measurements of the galaxy luminosity function, and better determinations of their kinematic properties and their relationship with the “great pancake” of bright satellites. It was originally suggested by Benson et al. (2002) (see also Kopev et al. 2007; Tollerud et al. 2008), that new surveys may reveal hundreds, if not thousands, of faint small satellites. However, it seems highly unlikely that the known population of bright Milky Way satellites will change significantly and thus that the conclusions of this paper – which pertain to the bright satellites – will be significantly altered.

ACKNOWLEDGMENTS

NIL is supported by the Minerva Stiftung of the Max Planck Gesellschaft.

REFERENCES

- Baugh C. M., Lacey C. G., Frenk C. S., Granato G. L., Silva L., Bressan A., Benson A. J., Cole S., 2005, MNRAS, 356, 1191
- Beloukhorov V., Zucker D. B., Evans N. W., Gilmore G., Vidrih S. et al 2006a, ApJ, 642, L137
- Beloukhorov V., Zucker D. B., Evans N. W., Wilkinson M. I., Irwin M. J. et al 2006b, ApJ, 647, L111
- Belokurov V., Zucker D. B., Evans N. W., Kleyna J. T., Kopev S. et al., 2007 ApJ, 654, 897
- Benson A. J., Frenk C. S., Lacey C. G., Baugh C. M., Cole S., 2002 MNRAS, 333, 177
- Brainerd T. G., 2005, ApJ, 628, 101
- Bower R. G., Benson A. J., Malbon R., Helly J. C., Frenk C. S., Baugh C. M., Cole S., Lacey C. G., 2006, MNRAS, 370, 645
- Bullock J. S., Kravtsov A. V., Weinberg D. H., 2000 ApJ, 539, 517
- Cole S., Lacey C. G., Baugh C. M., Frenk C. S., 2000 MNRAS, 319, 168
- Colless, M., et al. 2001 MNRAS, 328, 1039
- Diemand J., Kuhlen M., Madau P., 2007, ApJ, 667, 859
- Dinescu D. I., Keeney B. A., Majewski S. R., Girard T. M., 2004, AJ, 128,687
- Dinescu D. I., Girard T. M., van Altena W. F., López C. E., 2005, ApJ, 618,L25
- Gao L., Navarro J. F., Cole S., Frenk C. S., White S. D. M., Springel V., Jenkins A., Neto A. F., 2008 MNRAS 387, 536
- Grillmair C. J., 2006, ApJ, 645, L37
- Harker G., Cole S., Helly J. C., Frenk C. S., jenkins A., 2006 MNRAS, 367, 1039
- Helly J. C., Cole S., Frenk C. S., Baugh C. M., Benson A. J., Lacey C. G., 2003 MNRAS, 338, 903
- Holmberg E., 1969, ArA, 5, 305
- Ibata R. A., Wyse R. F. G., Gilmore G., Irwin M. J., Suntzeff N. B., 1997 AJ, 113, 634
- Kallivayalil N., van der Marel R. P., Alcock C., 2006a, ApJ, 652, 1213
- Kallivayalil N., van der Marel R. P., Alcock C., Axelrod T., Cook K. H., Drake A. J., Geha M., 2006b, ApJ, 638, 772
- Kang X., Mao S., Gao L., Jing Y. P., 2005, A&A, 437, 383
- Kaiser N., Ausser H., Burke B. E., Boesgaard H., Chambers K. et al, 2002 SPIE, 4836, 154
- Keller S. C., Schmidt B. P., Bessel M. S., Conroy P. G., Francis A. P. et al., 2007, PASA, 24, 1
- Klypin A., Kravtsov A. V., Valenzuela O., Prada F., 1999 ApJ, 522, 82
- Kopev S., Belokurov V., Eveans N. W., Hewett P. C., Irwin M. J., Gilmore G., Zucker D. B., Rix H-W., Fellhauer M., Bell E. F., Glushkova E. V., 2007, accepted by ApJ, *astrophysics preprints: astro-ph/0706.2687*
- Kroupa P., Theis C., Boily C. M., 2005, A&A, 431, 517
- Kunkel W. E., Demers S., 1976 RGOB, 182, 241
- Lacey C., Cole S., 1996, MNRAS, 281, 716
- Li, Y., Helmi, A., 2008, MNRAS, 385, 1365
- Libeskind N I., Cole S., Frenk C. S., Okamoto T., Jenkins A., 2007, MNRAS 374, 16
- Libeskind N I., Frenk C. S., Cole S. Helly J. C., Jenkins A. Navarro J. F., 2005, MNRAS
- Lynden-Bell D., 1976, MNRAS, 174, 695
- Lynden-Bell D., 1982, Obs, 102, 202
- Mateo M. L., 1998, ARA&A, 36 435
- Metz M., Kroupa P., 2007, MNRAS, 376, 387
- Metz M., Kroupa P., Jerjen H., 2009 MNRAS, accepted. preprint available at astro-ph/0901.1658
- Metz M., Kroupa P., Libeskind N I., 2008 ApJ, 680, 287
- Moore B., Ghinga S., Governato F., Lake G., Quinn T., Stadel J., Tozzi P., 1999 ApJ, 524, 19
- Navarro J F., Frenk C. S., White S. D. M., 1995, MNRAS, 275, 720
- Piatek S., Pryor C., Olszewski E. W., Harris H. C., Mateo M., et al. 2003, AJ, 126, 2346
- Piatek S., Pryor C., Bristow P., Olszewski E. W., Harris H. C., et al. 2005, AJ, 130, 95
- Piatek S., Pryor C., Bristow P., Olszewski E. W., Harris H. C., et al. 2006, AJ, 131, 1445
- Piatek S., Pryor C., Bristow P., Olszewski E. W., Harris H.

- C., Mateo M., Minniti, D., Tinney, C. G. 2007, AJ, 133, 818
- Sales L., Lambas D. G., 2004, MNRAS, 348, 1236
- Scholz R. D., Irwin M. J., 1994, IAU Symposium Vol 161, Astronomy from Wide-Field Imaging, ed. H. T. MacGillivray, 535
- Schwietzer A. E., Cudworth K. M., Majewski S. R., Suntzeff N. B., 1995 AJ, 110, 2747
- Schwietzer A. E., Cudworth K. M., Majewski S. R., 1997, in Astronomical Society of the Pacific Conference Series, Vol 127, Proper Motions and Galactic Astronomy, ed. R. M. Humphreys, 103
- Springel V. White S. D. M., Tormen G., Kauffmann G., 2001, MNRAS, 328, 726
- Springel V., 2005, MNRAS, 364, 1105
- Springel V., White S. D. M., Jenkins A., Frenk C. S., Yoshida N., Gao L., Navarro J., et al 2005 Nature 435, 620
- Springel V., Wang J., Vogelsberger M., Ludlow A., Jenkins A., Helmi A., Navarro F. F., Frenk C. S., White S. D. M., 2008 MNRAS, 391, 1685
- The Dark Energy Survey Collaboration, ArXiv Astrophysics pre-prints, astro-ph/0510346
- Tollerud E. J., Bullock J S., Strigari L. E., Willman B., submitted to ApJ, *astrophysics pre-prints*: astro-ph/0806.4381
- Willman B., Dalcanton J. J., Martinez-Delgado D., West A. A., Blanton M. R. et al, 2005, ApJ, 626, L85
- Yang X., Mo H. J., van den Bosch F. C, Weinmann S. M., Li C., Jing Y. P., 2005, MNRAS, 362, 711
- York D. G., Adelman J., Anderson J. E., Annis J., Bahcall N. et al 2000, AJ, 120, 1579
- Zaritsky D., Smith R., Frenk C. S., White S. D. M., 1997, ApJ, 478, 53
- Zentner A. R., Kravstov A V., Gnedin O Y., Klypin A. A., 2005, ApJ, 629, 219
- Zucker D. B, Belokurov V., Evans N. W., Wilkinson M. I., Irwin M. J. et al, 2006a ApJ, 643, L103
- Zucker D. B., Belokurov V., Evans N. W., Kleyana J. T., Irwin M. J. et al, 2006b ApJ, 650, L41